Energy & Environmental Science

Accepted Manuscript

ROYAL SOCIETY OF CHEMISTRY

www.rsc.org/ees

Broader context:

The fast development of polymer solar cells was made in last decades with the promises to eventually produce the light weight, flexible and low-cost clean energy alternatives. The prospect material innovation has long been a strong driving force to move the field forward. However, the development of electron acceptors experienced relatively slower pace than that of donor components. It is because the fullerene derivatives based acceptors are being widely used to in devices with no rivalry, though their obvious drawbacks, such as the limited chemical and energetic tunabilities, poor light-absorption, high-cost purification, morphology instability, have become the bottlenecks to constrain the further advancement of PSCs.

Recently, the exploration of non-fullerene electron acceptors is motivated, and we report herein the design of new non-fullerene acceptor, $SF(DPPB)_4$, which shows a cross-shaped molecular geometry to help suppressing strong intermolecular aggregation. Besides, the energy levels of $SF(DPPB)_4$ match well with those of P3HT, which allows not only achieving efficient exciton dissociation, but also ensure high V_{oc} (1.14 V) and efficiency (5.16%) in P3HT:$SF(DPPB)_4$ PSCs. Meanwhile, the devices show excellent thermal stability. The above results demonstrate that new design strategy to access high-performance non-fullerene acceptor would be promising for practical applications.

A PCE of 5.16% with a V_{oc} of 1.14 V is achieved for the thermally stable P3HT:SF(DPPB)$_4$ solar cells.

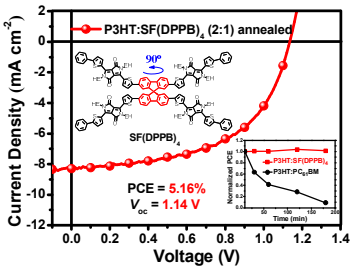

Journal Name

ARTICLE

A spirobifluorene and diketopyrrolopyrrole moieties based non-fullerene acceptor for efficient and thermally stable polymer solar cells with high open-circuit voltage

Received 00th January 20xx,
Accepted 00th January 20xx

DOI: 10.1039/x0xx00000x

www.rsc.org/

Shuixing Li,‡[a] Wenqing Liu,‡[a] Minmin Shi,*[a] Jiangquan Mai,[b] Tsz-Ki Lau,[b] Junhua Wan,[c] Xinhui Lu,[b] Chang-Zhi Li*[a] and Hongzheng Chen*[a]

In this work, we design and synthesize a new non-fullerene electron acceptor, SF(DPPB)$_4$, in which a spirobifluorene (SF) core is installed with four benzene endcapped diketopyrrolopyrrole (DPP) arms. SF(DPPB)$_4$ shows energy levels matching perfectly with those of the commonly used poly(3-hexyl thiophene) (P3HT) donor in polymer solar cells (PSCs). Furthermore, a designed cross-shaped molecular geometry helps suppressing the strong intermolecular aggregation in P3HT:SF(DPPB)$_4$ blend, leading to efficient non-fullerene PSCs. The resultant devices give a maximum power conversion efficiency (PCE) of 5.16% with an extremely high open-circuit voltage (V_{oc}) of 1.14 V. In contrast, the devices based on P3HT:PC$_{61}$BM blends provide a PCE of 3.18% with a V_{oc} of 0.62 V. Finally, we observe that the P3HT:SF(DPPB)$_4$ devices exhibit significantly improved thermal stability than the P3HT:PC$_{61}$BM ones: upon thermal treatment at 150 °C for 3 h, the PCEs of P3HT:SF(DPPB)$_4$ devices remain unchanged while those of the P3HT:PC$_{61}$BM devices drop drastically to below 1%. The above results demonstrate that new design strategy to access high-performance non-fullerene acceptor, SF(DPPB)$_4$, is promising for the future practical application of PSCs.

1. Introduction

Bulk heterojunction (BHJ) polymer solar cells (PSCs) have recently reached the power conversion efficiencies (PCEs) over 10%,[1-5] which are very attractive in the sense of their potentials allow being transformed into light-weight, flexible and low-cost photovoltaic technology.[6-8] However, current high-performance BHJs are dominantly made with the narrow band-gap polymer donors together with fullerene acceptors (e.g., [6,6]-phenyl-C$_{61}$/C$_{71}$-butyric acid methyl ester, PC$_{61}$BM and PC$_{71}$BM). Note that these two types of materials are relatively expensive. In addition to this, there are also some intrinsic drawbacks for fullerene materials, such as limited chemical and energetic tunabilities, poor light absorption, high production cost, and morphological instability, etc,[9-11] though fullerene acceptors exhibit high electron mobility, isotropic electron-transporting ability, and the capability of forming nanoscaled phase separation favorable for exciton dissociation.[12,13] It somehow becomes the bottleneck to constrain the material development for further advancing PSCs. Recent attentions have been paid to the development of non-fullerene acceptors.[14] It encouragingly shows that the PSCs based on non-fullerene electron acceptors allow exhibiting PCEs of 4-7%.[10,12,15-19]

Especially, those efficient BHJs made with a novel non-fullerene acceptor and economic polymers like poly(3-hexylthiophene) (P3HT) are attractive to some extent.[15,16,20-24] It is because that P3HT or poly(3-alkylthiophene) (P3AT) based block copolymers,[25-27] as a kind of low-cost and easy-process polymers, represent one of the most profoundly studied donor materials, showing a great potential to produce effective and low-cost PSCs. In order to pair well with the large band-gap donor, such as P3HT, new acceptors should have a high-lying energy levels, yet maintain suitable energetic difference with those of P3HT,[28] to simultaneously promote exciton dissociation and mitigate the potential loss to gain large open-circuit voltage (V_{oc}) for the device. On the other hand, the engineering of molecular geometry that could influence the blend morphology is the other crucial aspect. Recent works have proved that small molecule acceptors with twisted quasi-3D or 3D structures could be good candidates for achieving this in PSCs.[10,12,15,29-37] However, few researches report PSCs based on P3HT and a non-fullerene acceptor with PCEs over 3%.[15,16,23] Very recently, Zhan et al. reported an indacenodithiophene (IDT) unit based non-fullerene acceptor,

[a] MOE Key Laboratory of Macromolecular Synthesis and Functionalization, State Key Laboratory of Silicon Materials, & Department of Polymer Science and Engineering, Zhejiang University, Hangzhou 310027, P. R. China. Emails: minminshi@zju.edu.cn; czli@zju.edu.cn; hzchen@zju.edu.cn
[b] Department of Physics, Chinese University of Hong Kong, New Territories, Hong Kong, P. R. China
[c] Key Laboratory of Organosilicon Chemistry and Material Technology of Ministry of Education, Hangzhou Normal University, Hangzhou 310012, P. R. China

† Electronic Supplementary Information (ESI) available: Experimental details, density functional theory calculation details, two-dimensional GIWAXS details, ^{1}H NMR spectrum, ^{13}C NMR spectrum and Mass spectrum, TGA and DSC curves of SF(DPPB)$_4$, UV-vis absorption spectra of P3HT:SF(DPPB)$_4$ (2:1, by wt.) films with or without the thermal annealing at 120 °C for 10 min, $J^{0.5}$-V curves of the hole-only and electron-only devices based on P3HT:SF(DPPB)$_4$ films. See DOI: 10.1039/x0xx00000x

‡ These authors contribute equally to this work.

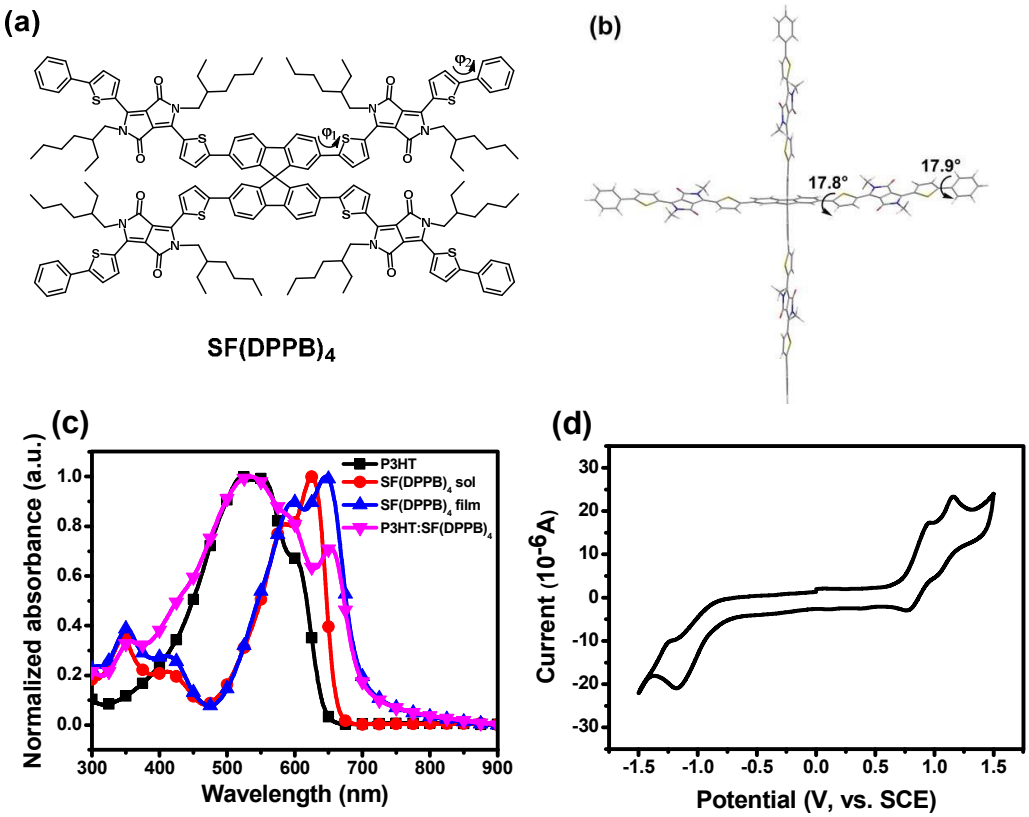

Fig. 1 (a) Chemical structure of $SF(DPPB)_4$; (b) ground-state geometry of $SF(DPPB)_4$ calculated by DFT method; (c) UV-vis absorption spectra of P3HT film, $SF(DPPB)_4$ solution and film, and P3HT:$SF(DPPB)_4$ (2:1, by wt.) blended film; (d) cyclic voltammogram for $SF(DPPB)_4$ in dichloromethane solution.

IDT-2BR, and the resulting PSCs based on P3HT:IDT-2BR blended films gave a PCE of 5.12%, which is the highest value for P3HT-based non-fullerene PSCs to date.[24] In our previous work, a non-fullerene acceptor, $F(DPP)_2B_2$, was developed through installing two benzene endcapped diketopyrrolopyrrole (DPP) onto a fluorene core. And it was found to possess relatively high electron mobility and suitable energy levels matching with those of P3HT. The P3HT:$F(DPP)_2B_2$ blend based PSCs provided a PCE of 3.17% with a very high V_{oc} of 1.18 V. Unfortunately, the above PSCs gave a small short-circuit current density (J_{sc}) of 5.35 mA cm^{-2}, which could be ascribed to large phase separation (40-60 nm) in the blended films.[38]

Taking the above considerations into accounts, we explore herein a new non-fullerene acceptor, $SF(DPPB)_4$ that is equivalent to the cross-shaped molecular configuration of two $F(DPP)_2B_2$ (Figure 1a). Because the two fluorene rings are perpendicular to each other in a spirofluorene (SF) core, the new $SF(DPPB)_4$ are less crystalline and can prevent from the forming of large aggregates when blended with P3HT to fabricated PSCs. It assures potential high exciton dissociation efficiency and large J_{sc} in device. In the meanwhile, the relatively high electron mobility and appropriate energy levels similar as $F(DPP)_2B_2$ are preserved for $SF(DPPB)_4$. After proper optimization of the device fabrication, we achieve a maximum PCE of 5.16% with a V_{oc} of 1.14 V, a J_{sc} of 8.29 mA cm^{-2}, and a fill factor (FF) of 0.55 for the PSCs based on P3HT:$SF(DPPB)_4$ blends. More importantly, the P3HT:$SF(DPPB)_4$ devices exhibit much better thermal stability than the P3HT:$PC_{61}BM$ ones: upon thermal treatment at 150 °C for 3 h, the PCEs of the P3HT:$SF(DPPB)_4$ devices remain unchanged while those of the P3HT:$PC_{61}BM$ devices drop drastically to below 1%.

2. Results and discussion

2.1. Synthesis and characterization of $SF(DPPB)_4$

$SF(DPPB)_4$ is synthesized via one-step palladium-catalyzed Suzuki coupling between tetra-boric ester functionalized SF and four brominated benzene-endcapped DPP units in good yield (80%). And its chemical structure is fully characterized by ^1H NMR, ^{13}C NMR, and MALDI-TOF MS (**Figs. S1-S3**, ESI†). Through density functional theory (DFT) calculations, the energy-optimized molecular geometry of $SF(DPPB)_4$ is shown, as expected, a cruciform configuration with two orthogonal conjugated backbones. Two dihedral angels between DPP and aromatic six-membered rings (fluorene and benzene), φ_1 and φ_2, are calculated as 17.8° and 17.9°, respectively (Fig. 1b). This

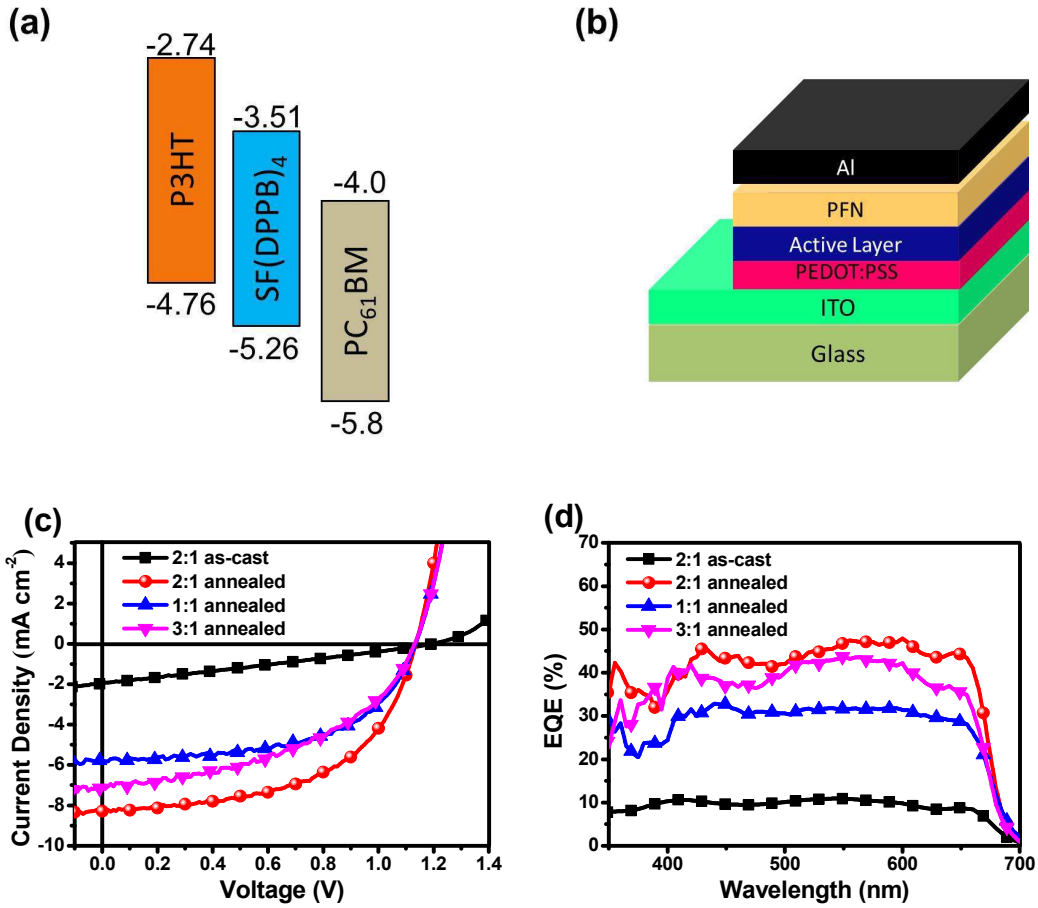

Fig. 2 (a) Energy levels of P3HT, $SF(DPPB)_4$ and $PC_{61}BM$; (b) the diagram of device structure; (c) *J-V* curves of PSCs with the structure of ITO/PEDOT:PSS/P3HT:$SF(DPPB)_4$/PFN/Al; (d) EQE spectra of P3HT:$SF(DPPB)_4$ based PSCs.

molecular arrangement prevents the strong intermolecular aggregation of $SF(DPPB)_4$, whereas maintain long and effective conjugation in each arm for photon harvest, and exposure sufficient π-surface for electron transport. Thermal properties are studied by thermogravimetric analysis (TGA) and differential scanning calorimetry (DSC). $SF(DPPB)_4$ shows excellent thermal stability with the decomposition temperature (T_d, 5% weight loss) of 403 °C under nitrogen atmosphere (**Fig. S4**, ESI†). As expected, we do not observe melting or crystallization peaks during the temperature range of 30~350 °C for $SF(DPPB)_4$ (**Fig. S5**, ESI†).

Fig. 1c depicts the UV-vis absorption spectra of $SF(DPPB)_4$ in $CHCl_3$ solution and thin film. A red-shift (21 nm) of the maximum absorption peak is observed from the solution to film, implying effective π-π stacking in the solid state. $SF(DPPB)_4$ film shows intense absorptions in the range of 550-700 nm, which are complement well with main absorptions of P3HT (400-600 nm). It suggests the excellent light-harvesting capability of the PSCs based on the P3HT:$SF(DPPB)_4$ blend. The cyclic voltammetry (CV) measurements are employed to estimate the energy level structure of $SF(DPPB)_4$. From the onset oxidation potential (0.86 V versus SCE) and the onset reduction potential (-0.89 V versus SCE) presented in **Fig. 1**d, the highest occupied molecular orbital (HOMO) and the lowest unoccupied molecular orbital (LUMO) energy levels of $SF(DPPB)_4$ are obtained as -5.26 and -3.51 eV, respectively. These values are close to those of $F(DPP)_2B_2$ (-5.21 and -3.39 eV),[38] implying that the replacement of fluorene with SF has minimal effect on the change of energy levels.

2.2. Photovoltaic property of P3HT:$SF(DPPB)_4$ blends

From the above results, we observe that, both HOMO and LUMO of $SF(DPPB)_4$ are sufficiently lower than those of P3HT (-4.76 and -2.74 eV), but significantly higher than those of $PC_{61}BM$ (-5.8 and -4.0 eV),[38] as illustrated in **Fig. 2**a. The offset between the LUMO of $SF(DPPB)_4$ and the HOMO of P3HT (1.25 eV) is much larger than that between $PC_{61}BM$ and P3HT (0.74 eV), which is favorable to achieve a high V_{oc} for the PSCs based on P3HT:$SF(DPPB)_4$ blends. It suggests that $SF(DPPB)_4$ is potentially an electron acceptor superior to $PC_{61}BM$ for the P3HT-based PSCs. Then, PSCs with P3HT as the electron donor and $SF(DPPB)_4$ as the electron acceptor are prepared, and the device structure is presented in **Fig. 2**b. **Fig. 2**c shows the current density-voltage (*J-V*) characteristics of the

Table 1 The photovoltaic performances of the PSCs based on P3HT:SF(DPPB)$_4$.

D:A (w/w)	V_{oc} (V)	J_{sc} (mA cm^{-2})	FF	PCE (%)
P3HT:SF(DPPB)$_4$ (2:1)[a]	1.20	1.91	0.28	0.63 (0.60)[d]
P3HT:SF(DPPB)$_4$ (1:1)[b]	1.13	5.78	0.57	3.70 (3.57)[d]
P3HT:SF(DPPB)$_4$ (2:1)[b]	1.14	8.29	0.55	5.16 (5.10)[d]
P3HT:SF(DPPB)$_4$ (3:1)[b]	1.13	7.13	0.46	3.68 (3.55)[d]
P3HT:PC$_{61}$BM (1:0.8)[c]	0.62	8.27	0.62	3.18 (3.14)[d]

[a] As-cast. [b] Annealed at 120 °C for 10 min. [c] Annealed at 170 °C for 10 min. [d] The values in the parentheses are the average PCEs from 10 devices.

PSCs under AM 1.5G illumination at an intensity of 100 mW cm^{-2}, and all photovoltaic data are summarized in **Table 1**. We can find that, thermal annealing can improve significantly the device performance. Without annealing, a poor PCE of 0.63% with a V_{oc} of 1.20 V, a J_{sc} of 1.91 mA cm^{-2}, and a FF of 0.28 is obtained when the blend weight ratio of donor (P3HT) and acceptor (SF(DPPB)$_4$) is 2:1. Upon thermal annealing at 120 °C for 10 min, the device with the same D:A blend ratio can give a maximum PCE of 5.16% with a V_{oc} of 1.14 V, a J_{sc} of 8.29 mA cm^{-2}, and a FF of 0.55. To our knowledge, this efficiency is one of the highest values ever reported for P3HT and non-fullerene acceptor based PSCs. PSCs with other weight ratios of P3HT and SF(DPPB)$_4$ (1:1 and 3:1) are also fabricated, but the decreased PCEs are observed than those of devices with the D:A weight ratio of 2:1. For comparison, the P3HT:PC$_{61}$BM device only provides a PCE of 3.18% with a V_{oc} of 0.62 V, a J_{sc} of 8.27 mA cm^{-2}, and a FF of 0.62. Apparently, the P3HT:SF(DPPB)$_4$ devices (with D:A weight ratio of 2:1 and annealing treatment) exhibit superior performance than that of fullerene based devices, which is mainly attributed to the particularly higher V_{oc}, and the reserved J_{sc} and FF. It is in the perfect agreement with the energy levels values from CV measurements. Shown in **Fig. 2**d is the external quantum efficiency (EQE) curves of P3HT:SF(DPPB)$_4$ based PSCs. It is obvious that the shapes of the EQE spectra resemble those of the sum of donor and acceptor absorptions, suggesting that each component in the active layers contributes to the photovoltaic responses.

2.3. Effects of thermal annealing on absorption and mobility

To understand the reasons for the performance improvement of the annealed devices, we record the UV-vis absorption spectra of P3HT:SF(DPPB)$_4$ films with or without annealing (**Fig. S6**, ESI†). After annealing, the absorptions for both P3HT and SF(DPPB)$_4$ are dramatically enhanced, implying that thermal annealing promote the improved molecular interaction, and perhaps molecular orientation. We also employ space charge limited current (SCLC) method to investigate the influences of thermal annealing on the charge-transporting properties of P3HT:SF(DPPB)$_4$ blended films. **Figs. S7** and **S8** show the $J^{0.5}$-V characteristics of the hole-only and electron-only devices taking the 2:1 P3HT:SF(DPPB)$_4$ films with or without the thermal annealing as the charge-transporting layers. From **Fig. S7**, the hole mobility of the as-cast blended film is calculated to be 8.65×10^{-5} cm^{2}V^{-1}s^{-1}, after annealing, the hole mobility increases to 14.80×10^{-5} cm^{2}V^{-1}s^{-1}. Similar change is also observed for the electron mobilities: thermal annealing can elevate the electron mobility from 6.70×10^{-5} to 12.92×10^{-5} cm^{2}V^{-1}s^{-1} (**Fig. S8**). Therefore, we speculate that, thermal annealing can promote intermolecular π-π stacking in the P3HT:SF(DPPB)$_4$ films, leading to stronger absorptions and better charge transport, which are responsible for the improvement of photovoltaic properties.

2.4. Influences of thermal annealing on molecular packing

Grazing-incidence wide-angle X-ray scattering (GIWAXS) measurements are further used to investigate the crystallinity and molecular orientation in both neat and blended films. The two-dimensional (2D) GIWAXS patterns are shown in **Fig. 3**, which presents the intensity profiles versus wave vector q_z and q_r, corresponding to the molecular arrangement order in out-of-plane and in-plane directions, respectively. It is found that the neat SF(DPPB)$_4$ films with or without the thermal annealing don't show any obvious diffraction peaks, which indicates that SF(DPPB)$_4$ is nearly amorphous, agreeing with the results from DSC measurements. On the contrary, the neat P3HT film shows a (100) lamellar diffraction peak centered at $q_z \approx 0.38$ Å^{-1} ($d \approx 16.5$ Å), consistent with previous studies.[39-41] After annealing, a much stronger (100) peak, even up to three orders of lamellar diffraction peaks for P3HT appear along q_z direction at $q_z \approx 0.38$, 0.76, and 1.14 Å^{-1}, corresponding to edge-on oriented P3HT domains. There is also one lamellar peak observed at $q_r \approx 0.36$ Å^{-1} ($d \approx 17.4$ Å), indicating the co-existence of face-on oriented domains in the annealed P3HT film. And the (010) π-π stacking diffraction peak is found to concentrate along q_z axis at $q_z \approx 1.65$ Å^{-1} ($d \approx 3.8$ Å), arising from the face-on oriented P3HT domains as well. For the P3HT:SF(DPPB)$_4$ blended film without annealing, we can only observe a lamellar diffraction peak $q_z \approx 0.35$ Å^{-1} ($d \approx 18.2$ Å). After the annealing of the P3HT:SF(DPPB)$_4$ blended film, the lamellar diffraction peaks corresponding to edge-on stacked P3HT domains are observed up to three orders along q_z axis at $q_z \approx 0.38$, 0.76, and 1.13 Å^{-1}. In the same time, face-on oriented P3HT domains give rise to a lamellar peak along q_r axis at $q_r \approx 0.36$ Å^{-1} ($d \approx 17.4$ Å) and a π-π peak along q_z axis at $q_z \approx 1.66$ Å^{-1} ($d \approx 3.8$ Å). The above results demonstrate no doubt that, annealing treatment can promote the crystallization and preferred face-on stacking of P3HT in the blended film, resulting in the much better light-harvesting and charge-transporting capabilities of the P3HT:SF(DPPB)$_4$ blended film. Thereby, the photovoltaic performances of the PSCs are elevated tremendously.

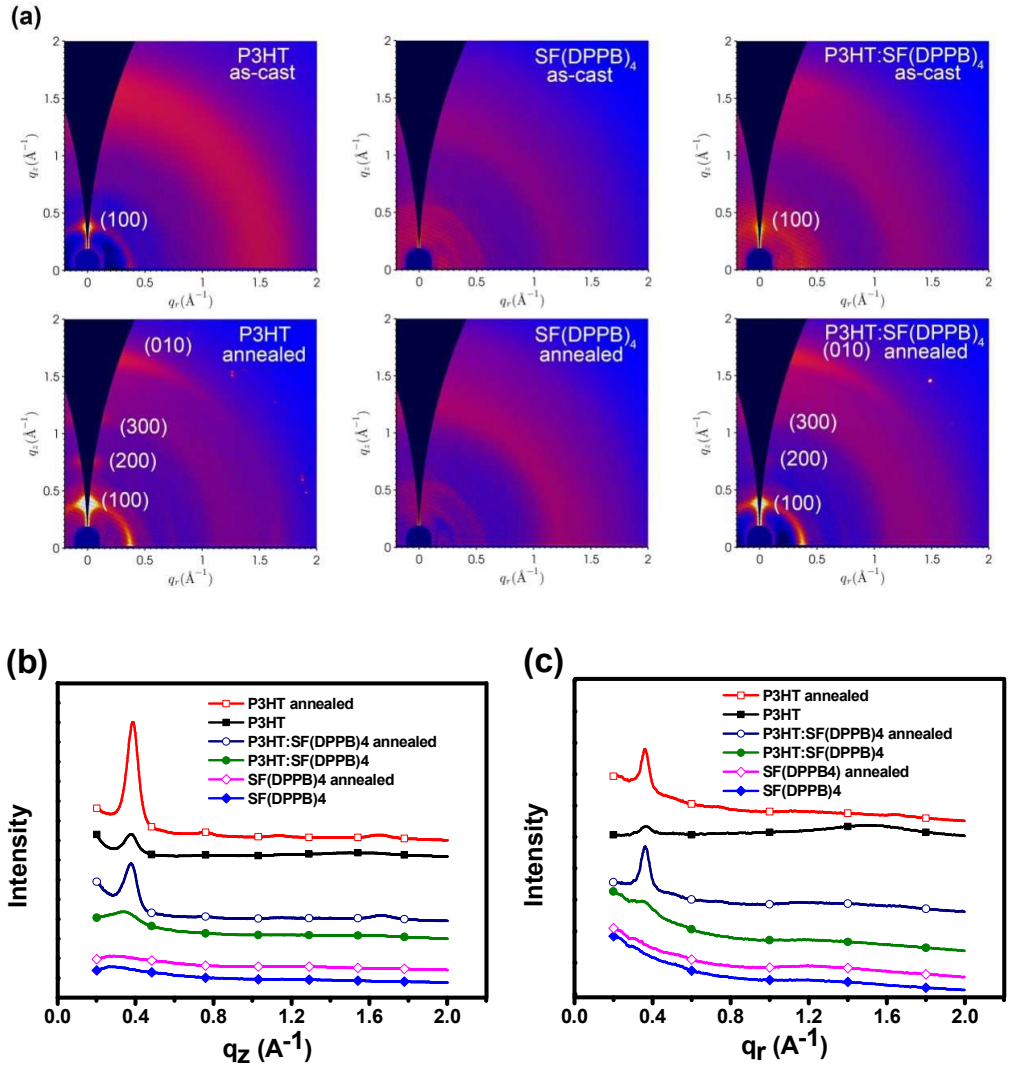

Fig. 3 (a) The 2D GIWAXS images of P3HT, SF(DPPB)$_4$ and 2:1 P3HT:SF(DPPB)$_4$ thin films with or without the thermal annealing at 120 °C for 10 min; (b) the intensity profiles along q_z axis of P3HT, SF(DPPB)$_4$ and 2:1 P3HT:SF(DPPB)$_4$ thin films; (c) the corresponding intensity profiles along q_r axis.

2.5. Morphology of P3HT:SF(DPPB)$_4$ films

The morphologies of the as-cast and annealed 2:1 P3HT:SF(DPPB)$_4$ blended films are studied by using atomic force microscopy (AFM) (**Fig. 4**). It can be seen that, in the as-cast film P3HT is completely compatible with SF(DPPB)$_4$, and the RMS roughness of the blended film is only 0.394 nm. After thermal annealing, due to the self-organization of P3HT and SF(DPPB)$_4$, the RMS roughness of the blended film increases to 0.633 nm. And the interconnected grains are identified at top-surface with the size of 20-30 nm, indicating the suitable-size of component domains and percolated network are formed. Thus, thermal annealing results in the enhanced photovoltaic performances. It is worth noting that, because of the cross-shaped molecular geometry of SF(DPPB)$_4$, the P3HT:SF(DPPB)$_4$ film exhibits much finer domains (20-30 nm) than that of previous P3HT:F(DPP)$_2$B$_2$ film (40-60 nm). This would play an important role to assure a higher exciton dissociation efficiency and a larger J_{sc} for the P3HT:SF(DPPB)$_4$ based PSCs. So the PCE is 5.16% for the P3HT:SF(DPPB)$_4$ based PSCs, instead, 3.17% for the P3HT:F(DPP)$_2$B$_2$ based PSCs.

2.6. Morphological and device stability

To explore the morphological stability of the P3HT:SF(DPPB)$_4$ and P3HT:PC$_{61}$BM blended films, optical microscopy is used to obtain the morphological images for the films with thermal treatment at 150 °C for different time (**Fig. 5**a). It is observed that the P3HT:PC$_{61}$BM films produce lots of micrometer-scaled aggregates after thermal treatment for only 0.5 h and the

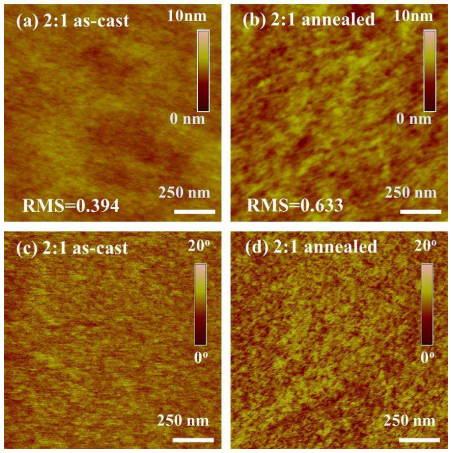

Fig. 4 AFM height (a, b) and phase (c, d) images of the as-cast (a, c) and annealed (b, d) P3HT:SF(DPPB)$_4$ films.

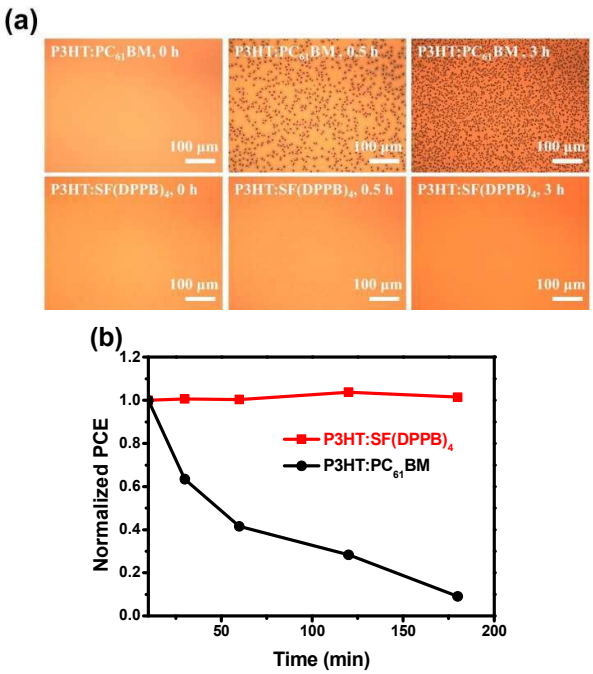

Fig. 5 (a) Morphological stability of P3HT:$PC_{61}BM$ (1:0.8, by wt.) and P3HT:SF(DPPB)$_4$ (2:1, by wt.) blended films after thermal treatment at 150 °C for different time. Images were captured by optical microscopy; (b) the stability of the PCEs for the devices based on P3HT:SF(DPPB)$_4$ (2:1, by wt.) and P3HT:$PC_{61}BM$ (1:0.8, by wt.) blended films after thermal treatment at 150 °C for different time.

aggregation becomes worse and worse with the extension of treating time. And the PCE of the corresponding device drops rapidly to below 1% after 3 h thermal treatment. These phenomena for the P3HT:$PC_{61}BM$ film and the related device are in agreement with previous work in references.[16,42] In contrast, due to the near amorphous nature of SF(DPPB)$_4$, the P3HT:SF(DPPB)$_4$ film remains homogenous morphology and no aggregates can be observed even after 3 h thermal treatment. As a result, the PCEs of the P3HT:SF(DPPB)$_4$ based device keep nearly steady during the thermal treatment (**Fig. 5**b). The excellent thermal stability in the morphology of P3HT:SF(DPPB)$_4$ film is inevitably favorable for the future practical application of SF(DPPB)$_4$ as the acceptor in the field of PSCs.

3. Conclusions

In summary, a spirobifluorene core based non-fullerene electron acceptor, SF(DPPB)$_4$, is designed and synthesized. SF(DPPB)$_4$ owns a cruciform molecular configuration, which assures fine phase separation in the active layer of PSCs. Besides, SF(DPPB)$_4$ also exhibits appropriate absorption bands and matched energy levels with P3HT. Owing to the good morphology and an outstandingly high V_{oc} of 1.14 V, the PSCs based on the P3HT:SF(DPPB)$_4$ blended films provide the best PCE of 5.16%. To the best of our knowledge, this PCE is one of the highest values reported in the literature to date for P3HT-based fullerene-free PSCs. And the P3HT:SF(DPPB)$_4$ based devices also show excellent thermal stability upon thermal treatment at 150 °C for up to 3 h, demonstrating that SF(DPPB)$_4$ is a promising non-fullerene acceptor in the future practical application of PSCs.

Acknowledgements

S. Li and W. Liu contribute equally to this work. M. Shi and H. Chen would like to gratefully acknowledge the financial support from the National Natural Science Foundation of China (Nos. 21474088, 51261130582, 91233114, 51561145001) and Zhejiang Province Natural Science Foundation (No. LR13E030001). The work was also partly supported by 973 program (No. 2014CB643503). J. Mai, T.-K. Lau and X. Lu acknowledge the financial support from Research Grant Council of Hong Kong (General Research Fund No. 2130394 and Theme-based Research Scheme No. T23-407/13-N).

Notes and references

1. Y. Liu, J. Zhao, Z. Li, C. Mu, W. Ma, H. Hu, K. Jiang, H. Lin, H. Ade and H. Yan, *Nat. Commun.*, 2014, **5**, 5293.
2. Z. He, B. Xiao, F. Liu, H. Wu, Y. Yang, S. Xiao, C. Wang, T. P. Russell and Y. Cao, *Nat. Photonics*, 2015, **9**, 174-179.
3. J.-D. Chen, C. Cui, Y.-Q. Li, L. Zhou, Q.-D. Ou, C. Li, Y. Li and J.-X. Tang, *Adv. Mater.*, 2015, **27**, 1035-1041.
4. X. Ouyang, R. Peng, L. Ai, X. Zhang and Z. Ge, *Nat. Photonics*, 2015, **9**, 520-524.
5. V. Vohra, K. Kawashima, T. Kakara, T. Koganezawa, I. Osaka, K. Takimiya and H. Murata, *Nat. Photonics*, 2015, **9**, 403-408.
6. G. Yu, J. Gao, J. C. Hummelen, F. Wudl and A. J. Heeger, *Science*, 1995, **270**, 1789-1791.
7. Y. Li, *Acc. Chem. Res.*, 2012, **45**, 723-733.
8. C. H. Duan, F. Huang and Y. Cao, *J. Mater. Chem.*, 2012, **22**, 10416-10434.

9. Y. He and Y. Li, *Phys. Chem. Chem. Phys.*, 2011, **13**, 1970-1983.
10. J. Zhao, Y. Li, H. Lin, Y. Liu, K. Jiang, C. Mu, T. Ma, J. Y. Lin Lai, H. Hu, D. Yu and H. Yan, *Energy Environ. Sci.*, 2015, **8**, 520-525.
11. C.-Z. Li, H.-L. Yip and A. K. Y. Jen, *J. Mater. Chem.*, 2012, **22**, 4161-4177.
12. Y. Liu, C. Mu, K. Jiang, J. Zhao, Y. Li, L. Zhang, Z. Li, J. Y. L. Lai, H. Hu, T. Ma, R. Hu, D. Yu, X. Huang, B. Z. Tang and H. Yan, *Adv. Mater.*, 2015, **27**, 1015-1020.
13. V. D. Mihailetchi, J. K. J. van Duren, P. W. M. Blom, J. C. Hummelen, R. A. J. Janssen, J. M. Kroon, M. T. Rispens, W. J. H. Verhees and M. M. Wienk, *Adv. Funct. Mater.*, 2003, **13**, 43-46.
14. Y. Lin and X. Zhan, *Mater. Horiz.*, 2014, **1**, 470-488.
15. Z. Mao, W. Senevirathna, J.-Y. Liao, J. Gu, S. V. Kesava, C. Guo, E. D. Gomez and G. Sauvé, *Adv. Mater.*, 2014, **26**, 6290-6294.
16. S. Holliday, R. S. Ashraf, C. B. Nielsen, M. Kirkus, J. A. Röhr, C.-H. Tan, E. Collado-Fregoso, A.-C. Knall, J. R. Durrant, J. Nelson and I. McCulloch, *J. Am. Chem. Soc.*, 2014, **137**, 898-904.
17. Y. Lin, Z.-G. Zhang, H. Bai, J. Wang, Y. Yao, Y. Li, D. Zhu and X. Zhan, *Energy Environ. Sci.*, 2015, **8**, 610-616.
18. Y. Lin, J. Wang, Z.-G. Zhang, H. Bai, Y. Li, D. Zhu and X. Zhan, *Adv. Mater.*, 2015, **27**, 1170-1174.
19. D. Sun, D. Meng, Y. Cai, B. Fan, Y. Li, W. Jiang, L. Huo, Y. Sun and Z. Wang, *J. Am. Chem. Soc.*, 2015, **137**, 11156-11162.
20. J. T. Bloking, X. Han, A. T. Higgs, J. P. Kastrop, L. Pandey, J. E. Norton, C. Risko, C. E. Chen, J. L. Bredas, M. D. McGehee and A. Sellinger, *Chem. Mater.*, 2011, **23**, 5484-5490.
21. Y. Zhou, Y.-Z. Dai, Y.-Q. Zheng, X.-Y. Wang, J.-Y. Wang and J. Pei, *Chem.Commun.*, 2013, **49**, 5802-5804.
22. Y. Kim, C. E. Song, S.-J. Moon and E. Lim, *Chem.Commun.*, 2014, **50**, 8235-8238.
23. G. D. Sharma, M. Anil Reddy, D. V. Ramana and M. Chandrasekharam, *RSC Adv.*, 2014, **4**, 33279-33285.
24. Y. Wu, H. Bai, Z. Wang, P. Cheng, S. Zhu, Y. Wang, W. Ma and X. Zhan, *Energy Environ. Sci.*, 2015, **8**, 3215-3221.
25. M. He, W. Han, J. Ge, Y. Yang, F. Qiu and Z. Lin, *Energy Environ. Sci.*, 2011, **4**, 2894-2902.
26. M. He, W. Han, J. Ge, W. Yu, Y. Yang, F. Qiu and Z. Lin, *Nanoscale*, 2011, **3**, 3159-3163.
27. W. Han, M. He, M. Byun, B. Li and Z. Lin, *Angew. Chem. Int. Ed.*, 2013, **52**, 2564-2568.
28. R. A. J. Janssen and J. Nelson, *Adv. Mater.*, 2013, **25**, 1847-1858.
29. Y. Lin, H. Wang, Y. Li, D. Zhu and X. Zhan, *J. Mater. Chem. A*, 2013, **1**, 14627-14632.
30. Y. Z. Lin, P. Cheng, Y. F. Li and X. W. Zhan, *Chem. Commun.*, 2012, **48**, 4773-4775.
31. H. Li, T. Earmme, G. Ren, A. Saeki, S. Yoshikawa, N. M. Murari, S. Subramaniyan, M. J. Crane, S. Seki and S. A. Jenekhe, *J. Am. Chem. Soc.*, 2014, **136**, 14589-14597.
32. Y. Lin, Y. Wang, J. Wang, J. Hou, Y. Li, D. Zhu and X. Zhan, *Adv. Mater.*, 2014, **26**, 5137-5142.
33. Y. Yang, G. Zhang, C. Yu, C. He, J. Wang, X. Chen, J. Yao, Z. Liu and D. Zhang, *Chem. Commun.*, 2014, **50**, 9939-9942.
34. H. Li, Y.-J. Hwang, B. A. E. Courtright, F. N. Eberle, S. Subramaniyan and S. A. Jenekhe, *Adv. Mater.*, 2015, **27**, 3266-3272.
35. Y. Liu, J. Y. L. Lai, S. Chen, Y. Li, K. Jiang, J. Zhao, Z. Li, H. Hu, T. Ma, H. Lin, J. Liu, J. Zhang, F. Huang, D. Yu and H. Yan, *J. Mater. Chem. A*, 2015, **3**, 13632-13636.
36. X.-F. Wu, W.-F. Fu, Z. Xu, M. Shi, F. Liu, H.-Z. Chen, J.-H. Wan and T. P. Russell, *Adv. Funct. Mater.*, 2015, **25**, 5954-5966.
37. S.-Y. Liu, C.-H. Wu, C.-Z. Li, S.-Q. Liu, K.-H. Wei, H.-Z. Chen and A. K. Y. Jen, *Adv. Sci.*, 2015, **2**, 4.
38. H. Shi, W. Fu, M. Shi, J. Ling and H. Chen, *J. Mater. Chem. A*, 2015, **3**, 1902-1905.
39. H. Kim, B. Yoon, J. Sung, D.-G. Choi and C. Park, *J. Mater. Chem.*, 2008, **18**, 3489-3495.
40. N. D. Treat, M. A. Brady, G. Smith, M. F. Toney, E. J. Kramer, C. J. Hawker and M. L. Chabinyc, *Adv. Energy Mater.*, 2011, **1**, 82-89.
41. E. Verploegen, C. E. Miller, K. Schmidt, Z. Bao and M. F. Toney, *Chem. Mater.*, 2012, **24**, 3923-3931.
42. C.-Z. Li, S.-C. Chien, H.-L. Yip, C.-C. Chueh, F.-C. Chen, Y. Matsuo, E. Nakamura and A. K. Y. Jen, *Chem. Commun.*, 2011, **47**, 10082-10084.